Published in final edited form as:
Neuroimage. 2012 May 1; 60(4): 2086–2095. doi:10.1016/j.neuroimage.2012.01.141.

Spatiotemporal mapping of brain atrophy in mouse models of Huntington's disease using longitudinal in vivo magnetic resonance imaging

Manisha Aggarwal[a,b,*], **Wenzhen Duan**[c], **Zhipeng Hou**[a], **Neal Rakesh**[a], **Qi Peng**[c], **Christopher A. Ross**[c,d,e], **Michael I. Miller**[b,f], **Susumu Mori**[a,g], and **Jiangyang Zhang**[a]

[a]Division of NMR Research, Department of Radiology; Johns Hopkins University School of Medicine, Baltimore, MD 21205

[b]Department of Biomedical Engineering; Johns Hopkins University School of Medicine, Baltimore, MD 21205

[c]Division of Neurobiology, Department of Psychiatry and Behavioral Sciences; Johns Hopkins University School of Medicine, Baltimore, MD 21205

[d]Departments of Neurology, Neuroscience and Pharmacology; Johns Hopkins University School of Medicine, Baltimore, MD 21205

[e]Program in Cellular and Molecular Medicine; Johns Hopkins University School of Medicine, Baltimore, MD 21205

[f]Center for Imaging Science; Johns Hopkins University School of Medicine, Baltimore, MD 21205

[g]F.M. Kirby Functional Imaging Center, Kennedy Krieger Institute, Baltimore, MD 21205

Abstract

Mouse models of Huntington's disease (HD), that recapitulate some of the phenotypic features of human HD, play a crucial role in investigating disease mechanisms and testing potential therapeutic approaches. Longitudinal studies of these models can yield valuable insights into the temporal course of disease progression and the effect of drug treatments on the progressive phenotypes. Atrophy of the brain, particularly the striatum, is a characteristic phenotype of human HD, is known to begin long before the onset of motor symptoms, and correlates strongly with clinical features. Elucidating the spatial and temporal patterns of atrophy in HD mouse models is important to characterize the phenotypes of these models, as well as evaluate the effects of neuroprotective treatments at specific time frames during disease progression. In this study, three dimensional in vivo magnetic resonance imaging (MRI) and automated longitudinal deformation-based morphological analysis was used to elucidate the spatial and temporal patterns of brain atrophy in the R6/2 and N171-82Q mouse models of HD. Using an established MRI-based brain atlas and mixed-effects modeling of deformation-based metrics, we report the rates of progression and region-specificity of brain atrophy in the two models. Further, the longitudinal analysis approach was used to evaluate the effects of sertraline and coenzyme Q_{10} (CoQ_{10}) treatments on progressive atrophy in the N171-82Q model. Sertraline treatment resulted in significant slowing of

[*]**Correspondence to:** Manisha Aggarwal Johns Hopkins University School of Medicine 334 Traylor Building, 720 Rutland Ave. Baltimore, MD 21205, USA Phone: (410) 955-9483 maggarw2@jhu.edu.

atrophy, especially in the striatum and frontal cortex regions, while no significant effects of CoQ_{10} treatment were observed. Progressive cortical and striatal atrophy in the N171-82Q mice showed significant positive correlations with measured functional deficits. The findings of this report can be used for future testing and comparison of potential therapeutics in mouse models of HD.

Keywords

Huntington's disease; mouse; longitudinal; brain atrophy; magnetic resonance imaging

Introduction

Huntington's disease (HD) is an autosomal dominant neurodegenerative disorder characterized by progressive motor, cognitive and behavioral dysfunction, with underlying neuropathology that includes selective neurodegeneration and atrophy, primarily in the striatum and cerebral cortex (Vonsattel et al., 1985; Walker, 2007; Ross and Tabrizi, 2011). Due to the progressive nature of HD, longitudinal monitoring of the disease is particularly important, in order to study its onset and progression and to evaluate the efficacy of therapeutic intervention. Recent longitudinal studies of HD patients with behavioral and imaging evaluation have shown great potential in achieving these goals (Paulsen et al., 2006; Aylward et al., 2010; Tabrizi et al., 2010; Aylward et al., 2011). Among the metrics frequently used in imaging evaluation, atrophy of the brain, particularly the striatum, is an important hallmark of HD, and is known to begin long before the onset of motor symptoms (Aylward et al., 2004).

Genetic mouse models of HD, that replicate certain phenotypic features of human HD, are instrumental for understanding the disease mechanisms, elucidating areas of the brain involved in structural and functional decline, and evaluating potential therapeutic approaches. There are different genetic mouse models used in HD studies (Menalled and Chesselet, 2002; Dedeoglu et al., 2003; Beal and Ferrante, 2004; Ramaswamy et al., 2007), and no single model is known to recapitulate the neuropathology of human HD in its entirety. Among the available mouse models, fragment HD models, including the R6/2 and N171-82Q lines, are widely used in preclinical trials since they exhibit multiple phenotypes and pathology resembling those of human HD, whereas full-length HD mouse models often have subtle phenotypes, making it less feasible to use them in short preclinical trials. Similar to the neuropathology of human HD, gross progressive atrophy of the brain is also a characteristic phenotype observed in mouse models of HD. Therapeutic trials in these models have shown potential benefits of a number of different treatment drugs, including sertraline, coenzyme Q_{10} (CoQ_{10}), minocycline, and remacemide (Ferrante et al., 2002; Stack et al., 2006; Peng et al., 2008). Longitudinal studies in genetic mouse models of HD can provide valuable insights into the spatial and temporal profiles of brain atrophy and how potential treatments affect these profiles. Conventionally, metrics of disease progression in mouse models of HD include behavioral testing for evaluation of functional impairment, and histology for neuropathology and structural atrophy. Histology, while contributing significantly to our understanding of the underlying pathology, cannot be used for monitoring structural atrophy over time. In the absence of reliable markers for longitudinal monitoring of neuropathological changes, there is sparse information on the dynamically varying spatial and temporal patterns of brain atrophy in these models.

In recent years, in vivo magnetic resonance imaging (MRI) is being increasingly used in longitudinal mouse studies (McDaniel et al., 2001; Lau et al., 2008; Ward et al., 2008; Maheswaran et al., 2009b). Previous MRI-based studies of mouse models of HD have been mostly cross-sectional, with analyses based on manual volumetry to quantitatively compare

gross structural volumes (Ferrante et al., 2002; Jenkins et al., 2005; Roberts et al., 2006; Sawiak et al., 2009) or deformation based automated morphological analysis (Lerch et al., 2008). Compared to manual volumetry, which relies on the accuracy of segmentation techniques, deformation based analysis (Ashburner et al., 1998) can provide a fully automated method for mapping and identifying progressive atrophy in the brain, requiring no *a priori* knowledge of the structures likely to be affected. It can capture certain well localized morphological changes, such as atrophy that occurs consistently in a specific cortical region among subjects, which may be difficult to identify by gross volumetric measurements. Two recent studies by our group have demonstrated the feasibility of longitudinal in vivo MRI and its use in detecting morphological differences between HD and wild-type mouse brains (Zhang et al., 2009; Cheng et al., 2011). With longitudinal imaging data, the parameters of interest include both group-wise morphological differences as well as time-dependent changes in brain morphology within each group, such as the spatiotemporally-varying rates of growth or atrophy.

In the present study, we combined an established MRI-based mouse brain atlas (Aggarwal et al., 2009) with longitudinal mixed effects modeling (Fitzmaurice et al., 2004) to investigate the spatiotemporal progression of brain atrophy in longitudinal MRI data acquired from two widely-used fragment mouse models of HD, the R6/2 and N171-82Q lines. The R6/2 is an early-onset model of HD, with a short life span of 12–16 weeks depending on the CAG size, and a well-studied progressive phenotype with gross striatal atrophy (Mangiarini et al., 1996; Stack et al., 2005). The R6/2 is the most commonly used transgenic mouse model of HD, and has also been used to screen for potential therapeutics. However, since the early disease onset and aggressive phenotypes in R6/2 mice make it difficult to use these mice in presymptomatic treatment trials, we used the N171-82Q model for evaluation of the effects of sertraline and CoQ_{10} treatments on the progression of brain atrophy. Compared to R6/2 mice, the N171-82Q is a late-onset model of HD, that displays relatively less aggressive phenotypes resembling human HD (Schilling et al., 1999). The adult-onset and prolonged time course of disease symptoms in N171-82Q mice allow a feasible experimental window for evaluating treatments presymptomatically as well as postsymptomatically, making it a useful model for therapeutic development (Hersch and Ferrante, 2004). Here, atlas-based mapping of longitudinal MR images and mixed-effects modeling of deformation based metrics allowed us to map the degree and rate of progression of brain atrophy in the R6/2 and N171-82Q models of HD, and investigate the effects of sertraline and CoQ_{10} treatments on the progression of regional atrophy in the N171-82Q model.

Material and Methods

Animals and treatment groups

All animal experiments were performed in accordance with the procedures approved by the Animal Research Committee at the Johns Hopkins University School of Medicine. Transgenic R6/2 mice were maintained by breeding heterozygous R6/2 males with females from their background strain (F1 of CBA x C57BL/6). Both male and female mice, with CAG repeat size ranging from 103 to 112 were used in the R6/2 study. For the N171-82Q study, transgenic N171-82Q mice were obtained by breeding heterozygous male N171-82Q mice with wild-type females from their background strain (B6C3F1). Only male mice with CAG repeat size of 82 were included in the N171-82Q study, since significant gender-based variability in N171-82Q mice has been previously reported (Duan et al., 2004). Genotyping of the offspring and determination of the CAG repeat size was performed by PCR assay on tail DNA (Laragen Inc., Los Angeles, CA, USA). For each study, wild-type (WT) littermate mice were used as controls. Starting at 6 weeks of age, the transgenic N171-82Q mice were divided into four treatment groups: vehicle-treated with daily intraperitoneal (i.p.) injection of 0.2% Tween-80 (n=6), sertraline-treated with daily i.p. injection of sertraline (10 mg/kg,

Toronto Research Chemicals, Canada) dissolved in 0.2% Tween-80 (n=8), CoQ_{10}-treated with 1% CoQ_{10} (Kaneka Corporation, Pasadena, TX, USA) supplemented in the chow (n=6), and combination-treated with both sertraline via daily i.p. injection and CoQ_{10} supplemented in the chow (n=8). The mice were housed in cages in groups of 3–5 on a 12 h light/dark cycle with *ad libitum* access to food and water. Table 1 summarizes the groups of animals used in this study.

In vivo MRI

Since the R6/2 is an early-onset model of HD, serial in vivo MR images of the R6/2 and age-matched control mouse brains were acquired starting at 3 weeks of age. To account for the rapid brain growth during the early postnatal phase, images were acquired weekly up to 6 weeks of age, and thereafter biweekly up to 12 weeks of age. For the N171-82Q model, which is an adult-onset model of HD, the transgenic and control mice were imaged starting at 6 weeks of age with subsequent scans at 10 and 14 weeks of age. Longitudinal imaging of these mice and measurements of structural volumes were reported previously (Zhang et al., 2009; Cheng et al., 2011) and are briefly described here. All in vivo MRI studies were performed on a horizontal-bore 9.4 Tesla NMR spectrometer (Bruker Biospin, Billerica, MA, USA), equipped with an animal imaging probe and a physiological monitoring system to monitor the ECG, respiration rate and body temperature. A 40-mm diameter birdcage coil was used as the RF transmitter and receiver. Three dimensional T2-weighted images were acquired using a fast spin echo (FSE) sequence with an echo time (TE) of 40 ms, pulse repetition time (TR) of 700 ms, echo train length of 4, flip angle of 40°, two signal averages, and native spatial resolution of $0.1 \times 0.1 \times 0.25$ mm^3. The imaging time was about 50 minutes per mouse. During imaging, mice were anesthetized with 1% isoflurane mixed with oxygen and air (1:3 ratio) via a vaporizer. The ambient temperature was maintained at 30°C throughout the scan via a heating block built into the gradient system.

Generation of strain-specific reference brain atlases

To establish a common coordinate space for spatial normalization and analysis of the longitudinal in vivo images, reference brain atlases based on the background strains for each model were generated. For the R6/2 model, a population-averaged MR brain atlas based on T2-weighted in vivo images from C57BL/6 mice (n=9, 12 week old) was used as the reference template. For the N171-82Q study, the wild-type control cohort (n=10, 6 week old) was used to create a background strain-specific reference atlas for image mapping. The details of the atlas generation procedure have been described in (Kovacevic et al., 2005; Aggarwal et al., 2009). Briefly, signals from non-brain tissue in the images were manually removed (skull stripping). The brain image of one mouse, with brain volume close to the median value of the control population, was chosen as the reference (I_0) for initialization of the atlas generation algorithm. The brain images were intensity-normalized and rigid aligned to I_0, and the voxel-wise mean of the aligned images was computed to generate an averaged template (I_1). This I_1 template was used for affine transformation of the individual images, and the affine-transformed images were then averaged to generate the template for the next step (I_2). The single-subject images were then warped to the averaged template I_2 using nonlinear transformations generated by large deformation diffeomorphic metric mapping (LDDMM), which generates topology-conserving diffeomorphic transformations that map the morphological differences between the reference template and each brain image in the form of deformation vector fields (Miller et al., 2002). This procedure was repeated until the averaged image generated by subsequent iterations revealed no visible change. The warped images from individual subjects were then averaged to generate the reference brain atlas. Segmentation and labeling of major brain structures in the reference brain atlas were performed according to (Aggarwal et al., 2009).

Diffeomorphic mapping to the reference atlas

Serial MR images of the transgenic and wild-type mice in each study were manually skull-stripped using the DiffeoMap software (www.mristudio.org), and aligned to the background strain-specific reference atlas using a rigid transformation model with six degrees of freedom. Intensity normalization of the aligned images to the reference atlas was done using a piece-wise linear function to equalize the mean intensities of the white matter, grey matter and cerebrospinal fluid regions. The normalized images were then nonlinearly warped to the reference atlas using intensity-based transformations generated by LDDMM. For longitudinal analysis of morphological changes, Jacobian maps of the transformations generated by LDDMM were computed for each subject at each time point. The determinant of the Jacobian provides a quantitative metric for measuring the local, voxel-wise shrinkage or expansion of the subject image relative to the reference atlas (Toga and Thompson, 2003). The Jacobian determinant was transformed to logarithmic scale (referred to as log-Jacobian in the following sections) to better approximate a normal distribution in order to allow the use of mixed-effects models for statistical analysis.

Longitudinal statistical analysis

Longitudinal local volumetric changes at each brain voxel, as measured by the derived log-Jacobian values, were modeled using linear mixed effects (LME) models. Because repeated measurements from the same subjects cannot be treated as independent observations, standard regression techniques are not valid for longitudinal data. LME models were used since they include a subset of the regression parameters as random effects, thereby accounting for the intra-subject covariance (Pinheiro and Bates, 2000). Longitudinal modeling of voxelwise log-Jacobian was carried out using LME models with age, genotype, and interaction between age and genotype, (and interaction between age and treatment, for the N171-82Q model) as the independent variables. For the R6/2 study, a linear splines model with a knot at 5 weeks of age was used:

$$Y_{ij}=\beta_1+\beta_2 t_{ij}+\beta_3\left(t_{ij}-5\right)_+ +\beta_4 G_i+\beta_5 t_{ij} G_i+\beta_6\left(t_{ij}-5\right)_+ G_i+b_{1i}+b_{2i}t_{ij}+\varepsilon_{ij} \quad [1]$$

which included fixed effects for age (β_2 and β_3), genotype (β_4), and the interaction of age with genotype (β_5 and β_6), and random intercept (b_{1i}) and slope (b_{2i}) terms to account for within-subject variability. t_{ij} denotes the age (in weeks) of the i^{th} subject at the j^{th} observation, G_i denotes the genotype (0 for wild-type, 1 for R6/2 transgenic) and ε_{ij} is the residual error term. The term $(t_{ij}\text{-}5)_+$ is equal to $(t_{ij}\text{-}5)$ when $t_{ij} > 5$, and equal to zero otherwise. Since brain growth in the mouse is known to continue during the early postnatal phase, we used linear splines to allow modeling of different rates of change for different age spans during the course of the study. For the N171-82Q study, the log-Jacobian values were fit to the following LME model:

$$Y_{ij}=\beta_1+\beta_2 t_{ij}+\beta_3 G_i+\beta_4 t_{ij} veh+\beta_5 t_{ij} CoQ_i+\beta_6 t_{ij} ser_i+\beta_7 t_{ij} comb_i+b_{1i}+b_{2i}t_{ij}+\varepsilon_{ij} \quad [2]$$

which included fixed effects for age (β_2), genotype (β_3), and interaction between age and treatment (β_4, β_5, β_6 and β_7), as well as random intercept (b_{1i}) and slope (b_{2i}) terms. G_i denotes the genotype (0 for wild-type, 1 for N171-82Q transgenic), and veh_i, CoQ_i, ser_i and $comb_i$ denote the treatment group (1 for vehicle-, CoQ_{10}-, sertraline- and combination-treated mice respectively, and 0 otherwise). Voxel-wise statistical testing for the estimated fixed effects parameters was based on the Wald statistic compared to a *t*-distribution with the degrees of freedom associated with each test (Fitzmaurice et al., 2004). To avoid Type I errors, the resulting statistical maps were corrected for multiple comparisons using the false discovery rate (FDR) set at 0.05 (Genovese et al., 2002). The longitudinal statistical analysis software was implemented in Matlab 7.5 (Mathworks Inc., Natick, MA).

Behavioral testing

Motor performance of the N171-82Q and wild-type littermate mice was assessed at 6, 10 and 14 weeks of age using a rotarod apparatus (Columbus Instruments, Columbus, OH), in which the time the mouse remains on the rod at accelerating speeds from 4 to 40 rpm was measured. The rotarod is a widely-used test designed to monitor motor coordination in mice (Jones and Roberts, 1968). Each mouse was initially trained for 5 min followed by a 1-hour rest period. Mice were then placed back on the rotarod for three trials (each of maximum 5 min and separated by a 30-min rest period) at accelerating speeds of 4 to 40 rpm. Testing was performed on three consecutive days, by which time a steady baseline level of performance was attained. The mean score of the trials on the three testing days was used for statistical analysis. Pearson's product correlation coefficient was used to test for association between imaging and behavioral measures.

Results

Longitudinal monitoring of morphological changes in the wild-type mouse brains

Longitudinal MRI of the WT cohorts showed that morphological changes in the mouse brains were dynamic and spatially non-uniform (Figure 1). Significant and rapid increase in local tissue volume as measured by the derived log-Jacobian maps was observed in the CBA × C57BL/6 mouse brains up to 5 weeks of age, in several regions including areas in the cerebellum, dorsal striatum and hippocampus, while a large part of the thalamus and ventral striatum showed no significant change. From 5 to 12 weeks, the dorsal striatum and hippocampus still showed significant increase in local tissue volume, but at a much lower rate than before. Similar patterns were found in the B6C3F1 mice between 6 to 14 weeks of age. The olfactory bulbs in CBA × C57BL/6 and B6C3F1 mice were found to undergo moderate but significant local volumetric increase in all age spans included in this study. The lateral ventricles also showed significant enlargement throughout up to 14 weeks of age. Significant progressive decrease in local tissue volume, as indicated by a negative rate of change of log-Jacobian values with age, was observed in several cortical regions (Figure 1).

Longitudinal monitoring of brain atrophy in the mouse models of HD

Our longitudinal data showed progressive and region-specific atrophy in the two mouse models studied here. To distinguish changes associated with atrophy in the R6/2 brains from those due to normal growth and maturation of the WT brains shown in Figure 1, differences in the rates of change of log-Jacobian between groups (age × genotype interaction) were examined (Figure 2). At 3 weeks of age, the R6/2 mice showed no significant atrophy in the brain compared to the WT cohort. From 3 to 5 weeks of age, the rate of atrophy was the highest in the neocortex and piriform cortex (with significant differences from the WT cohort), while the rest of the brain showed only mild or no atrophy. From weeks 5 to 12, regions in the striatum, thalamus, hippocampus and piriform cortex had significant rates of atrophy (Figure 2), whereas the cortical regions did not show significant progression of atrophy in this phase.

Compared to the R6/2 model, the N171-82Q mice showed a relatively late onset of brain atrophy (Figure 3), with no significant differences from the WT cohort observed at 6 weeks of age. After 6 weeks, significant progression of atrophy in the N171-82Q mice was detected in brain regions including the neocortex, striatum, hippocampus, piriform cortex and amygdala (Figure 3).

Treatment effects on brain atrophy in the N171-82Q mouse brain

To evaluate the effects of sertraline, CoQ_{10}, and combination of sertraline and CoQ_{10} treatments on atrophy in the N171-82Q model of HD, differences in the rates of change of

log-Jacobian between the treatment and sham (vehicle-treated) cohorts were examined. Longitudinal log-Jacobian analysis showed that sertraline treatment resulted in significant slowing of the progression of atrophy in the N171-82Q mouse brain, as the rate of atrophy in the sertraline-treated group was significantly lower compared to the vehicle-treated group, and this decrease in atrophy was localized to the striatum and frontal cortex regions (Figure 4). No treatment effect was observed in the piriform cortex or amygdala, areas that also showed progressive tissue atrophy in this model. We found no significant effect of CoQ_{10} treatment on regional atrophy in the N171-82Q brain (data not shown). Mice treated with a combination of sertraline and CoQ_{10} also showed significant decrease in the rate of atrophy compared to the vehicle-treated group, and the brain regions with significant treatment response were similar for both sertraline and combination treatments (Figure 4). Statistical testing for differences in regional atrophy between the sertraline- and combination-treated cohorts showed no significant differences between the two treatments.

Correlation of structural atrophy with functional outcome

To determine if there is an association between progressive structural atrophy and behavioral phenotype deficits in the N171-82Q mice, we evaluated the correlation between rotarod performance scores and structural volume measures from MRI. The rotarod scores correlated positively with cortical and striatal volumes at 14 weeks in N171-82Q transgenic mice ($r=0.557$, $p=0.007$ and $r=0.494$, $p=0.02$, respectively), but not in WT mice (Figure 5 A, B). There was a relatively stronger correlation between the rotarod scores at 14 weeks and the relative changes in cortical and striatal volumes in N171-82Q mice from 6 to 14 weeks of age ($r=0.797$, $p<0.0001$ and $r=0.723$, $p<0.0001$, respectively) (Figure 5 C, D). Further, to evaluate if attenuation of regional atrophy with sertraline and combination treatments had an association with functional improvement in N171-82Q mice, we manually selected a region of interest (ROI) within the frontal cortex and striatum, where significant treatment effect was detected based on log-Jacobian analysis (as shown in Figure 4). There was a strong positive correlation between the 14 week rotarod scores and the relative change in Jacobian values from 6 to 14 weeks of age averaged over the selected ROI ($r=0.809$, $p<0.0001$) (Figure 5 E). These results indicate that progressive tissue atrophy in the cortex and striatum correlates with the severity of motor symptoms in the N171-82Q model of HD, and both functional and imaging measures provide complementary metrics to evaluate and grade disease severity and treatment response in this model.

Discussion

The findings of the present study demonstrate the potential of longitudinal deformation-based morphological analysis of in vivo MR images to elucidate the complex spatiotemporal dynamics of age-related growth and progression of structural atrophy in the brain. The mouse brain is known to undergo age-related morphological changes, especially in the early postnatal phase that is characterized by rapid structural growth and development (Wingert, 1969; Chuang et al., 2011). Similar to the findings of our study, volumetric increases with age in the hippocampus, olfactory bulbs, ventricles and cerebellum, as well as age-related reduction in volume in the cerebral cortex have been reported in previous MRI-based longitudinal studies in different wild-type mouse strains (Lau et al., 2008; Maheswaran et al., 2009a; Maheswaran et al., 2009b). Elucidating the growth patterns of normal mouse brains will facilitate further understanding of how brain development in transgenic mouse models deviates from normal development.

Our findings in the R6/2 and N171-82Q mouse models of HD are consistent with the known pathological findings in these models. The R6/2 is a juvenile onset model of HD, with neuropathological symptoms reported as early as 30 days of age (Stack et al., 2005). In the present study, we observed significant and widespread brain atrophy that began around 3

weeks of age, and progressed to regions including the cortex, striatum, hippocampus, thalamus and piriform cortex (Figure 2). Although the exact mechanisms of neuronal degeneration in this model are not fully understood, detailed histological analyses have shown evidence of neurodegeneration occurring in the striatum, cortex and hippocampus (Iannicola et al., 2000; Turmaine et al., 2000; Ferrante et al., 2003), while differences in overall structural volumes in these regions between R6/2 and wild-type mice have also been reported by ex vivo high resolution MRI (Sawiak et al., 2009). Compared to the R6/2 mice, the N171-82Q model of HD has a longer N-terminal fragment of huntingtin and shows a relatively delayed onset of disease symptoms (Beal and Ferrante, 2004). Histology-based studies in this model have reported neuronal degeneration in the cortex, striatum, amygdala, hippocampus and piriform cortex (Saydoff et al., 2006). Significant progressive atrophy in these brain regions was detected in N171-82Q mice in the present study (Figure 3).

With longitudinal morphological analysis, we were able to estimate the rate of progressive atrophy throughout the brain in the R6/2 model from 3–12 weeks of age. An interesting observation in the present study was that significant progressive atrophy in the R6/2 cortex was observed predominantly in the early postnatal phase up to 5 weeks of age, and was relatively less evident in later stages (Figure 2). Our observation in the R6/2 mice is in contrast to clinical observations in human HD, where cortical atrophy has been observed towards later stages of the disease (Aylward et al., 1998). In comparison, progressive atrophy in other brain regions in R6/2 mice, e.g., the striatum and thalamus, was observed mainly after 5 weeks of age. Using toluidine blue staining, a study by Stack et al. has reported progressive increase in the number of degenerating neurons in the R6/2 striatum from 5 to 12 weeks of age (Stack et al., 2005).

We also demonstrated the use of longitudinal analysis to examine effects of different treatments on progressive brain atrophy. Significant decrease in the rate of progressive atrophy was observed in N171-82Q mice treated with sertraline, primarily in the striatum and frontal cortex regions. Sertraline is an antidepressant drug belonging to the class of selective serotonin reuptake inhibitors (SSRIs), that has been shown to have neuroprotective effects in HD mice by increasing brain-derived neurotrophic factor (BDNF) and neurogenesis (Peng et al., 2008). Previous histology-based studies have demonstrated amelioration of striatal atrophy and improved motor performance in N171-82Q mice treated with sertraline (Duan et al., 2008). While the effect of sertraline treatment on progressive cortical atrophy observed in the current study remains to be investigated by histological analysis, these findings indicate that imaging measures can provide sensitive metrics for longitudinal evaluation of disease severity and therapeutic response in mouse models of HD. In the present study, we observed no significant effect of CoQ_{10} treatment on the rate of progressive atrophy in N171-82Q mice and no significant difference between sertraline treatment and the combined treatment. CoQ_{10}, a cofactor in the mitochondrial electron transport chain and a potent antioxidant, had been shown to have therapeutic effects in mouse models of HD in previous studies. While CoQ_{10} treatment has been shown to attenuate weight loss in N171-82Q mice, there was no increase in survival or alteration of neurodegenerative processes in the brain (Schilling et al., 2001). Given these findings, further studies with a larger cohort size may be necessary to derive conclusive evidence of the effects of CoQ_{10} in this model. These results indicate that the longitudinal morphological analysis approach can be potentially used to analyze and compare the effects of different treatments quantitatively.

In this study, we found significant correlation between cortical and striatal atrophy and motor deficits in the N171-82Q model of HD. As seen from the findings in Figure 5, in the N171-82Q cohorts treated with sertraline and combination treatments, there was amelioration of regional atrophy in the cortex and striatum, and these mice also exhibited

decreased motor dysfunction. These findings suggest that functional deficits in this model, as evidenced from a decrease in the time spent on the rotarod, may be a consequence of progressive neuronal atrophy and loss of tissue volume in the cortex and striatum. Furthermore, rotarod scores in N171-82Q mice showed a stronger correlation with the changes in cortical and striatal volumes from 6 to 14 weeks of age, as compared to volumes measured at 14 weeks (Figure 5). This difference reflects the existent morphological variability in the mouse brain, and indicates that longitudinal measurements of volumetric changes over time, that are not affected by inter-subject variability, may be more reliable and sensitive metrics for assessment of disease severity in mouse models of HD, as compared to cross-sectional measurements.

It is necessary to point out some limitations of our approach. First, we used LME models with linear splines to model the voxel-wise longitudinal changes in log-Jacobian in the whole brain. However, different regions in the brain may differ in growth and maturation profiles, for instance local volumetric measures at specific cortical regions in the present study were observed to peak at 4 weeks of age, suggesting that a single model may not be optimal to model the growth profiles of all structures in the brain. Future studies for mapping growth profiles in the brain may thus require more complex region-specific models to appropriately represent the changing structural morphologies. Second, the accuracy of our approach is determined by the level of accuracy of image mapping and the spatial variability in the locations of HD-related morphological changes among subjects. A good example is the lateral ventricles. Enlargement of the ventricles has conventionally been used as an index of pathological damage in HD. As seen in Figure 2, local volumetric enlargement in the R6/2 mice compared to WT controls was also observed in the present study in the 5 to 12 week age span, but these differences did not reach statistical significance. The dramatic change in ventricular shapes and its variability often pose a challenge for analysis based on image mapping to capture, as shown in Zhang et al. (2009). In the future, further improvement in the accuracy of our image mapping techniques may be necessary to enhance the sensitivity of the longitudinal analysis approach to capture such variability in morphological changes. Third, serial in vivo MRI of the WT and transgenic mice in this study required the animals to undergo anesthesia at the experimental time points. Some previous studies have shown potential effects of anesthetic exposure during early development in mice and rats in regards to neurohistopathological changes, including the potency of isoflurane to cause neurodegeneration in neonatal mice (Jevtovic-Todorovic et al., 2003; Liang et al., 2010). Since the precise effects of anesthesia at subsequent postnatal stages on morphological changes in the brain are not completely understood, the effects of anesthetic exposure on the longitudinal morphological findings in the present study cannot be ruled out.

To summarize, in this study longitudinal analysis based on in vivo MRI was applied to elucidate the spatiotemporal progression of brain atrophy in the R6/2 and N171-82Q mouse models of HD. The findings presented here will be important for future testing of potential therapeutics in these models of HD, and the techniques can also facilitate relatively high-throughput automated anatomical phenotyping in other mouse models of neurodegenerative disorders. The ability to follow the progression of brain atrophy longitudinally in mouse models will aid our understanding of these disorders and facilitate testing the efficacy of pharmacological intervention.

Acknowledgments

This research was supported by grants from the CHDI Inc. foundation (to W. Duan), NINDS NS16375 (to CAR), NIH EB003543, RR15241, and ES012665 (to S. Mori), and NIHNS065306 (to J. Zhang).

References

Aggarwal M, Zhang J, Miller MI, Sidman RL, Mori S. Magnetic resonance imaging and micro-computed tomography combined atlas of developing and adult mouse brains for stereotaxic surgery. Neuroscience. 2009; 162(4):1339–1350. [PubMed: 19490934]

Ashburner J, Hutton C, Frackowiak R, Johnsrude I, Price C, Friston K. Identifying global anatomical differences: deformation-based morphometry. Hum Brain Mapp. 1998; 6(5–6):348–57. [PubMed: 9788071]

Aylward EH, Anderson NB, Bylsma FW, Wagster MV, Barta PE, Sherr M, Feeney J, Davis A, Rosenblatt A, Pearlson GD, Ross CA. Frontal lobe volume in patients with Huntington's disease. Neurology. 1998; 50(1):252–8. [PubMed: 9443488]

Aylward EH, Liu D, Nopoulos PC, Ross CA, Pierson RK, Mills JA, Long JD, Paulsen JS. Striatal Volume Contributes to the Prediction of Onset of Huntington Disease in Incident Cases. Biol Psychiatry. 2011

Aylward EH, Nopoulos PC, Ross CA, Langbehn DR, Pierson RK, Mills JA, Johnson HJ, Magnotta VA, Juhl AR, Paulsen JS. Longitudinal change in regional brain volumes in prodromal Huntington disease. J Neurol Neurosurg Psychiatry. 2010; 82(4):405–10. [PubMed: 20884680]

Aylward EH, Sparks BF, Field KM, Yallapragada V, Shpritz BD, Rosenblatt A, Brandt J, Gourley LM, Liang K, Zhou H, Margolis RL, Ross CA. Onset and rate of striatal atrophy in preclinical Huntington disease. Neurology. 2004; 63(1):66–72. [PubMed: 15249612]

Beal MF, Ferrante RJ. Experimental therapeutics in transgenic mouse models of Huntington's disease. Nat Rev Neurosci. 2004; 5(5):373–84. [PubMed: 15100720]

Cheng Y, Peng Q, Hou Z, Aggarwal M, Zhang J, Mori S, Ross CA, Duan W. Structural MRI detects progressive regional brain atrophy and neuroprotective effects in N171-82Q Huntington's disease mouse model. Neuroimage. 2011; 56(3):1027–34. [PubMed: 21320608]

Chuang N, Mori S, Yamamoto A, Jiang H, Ye X, Xu X, Richards LJ, Nathans J, Miller MI, Toga AW, Sidman RL, Zhang J. An MRI-based atlas and database of the developing mouse brain. Neuroimage. 2011; 54(1):80–9. [PubMed: 20656042]

Dedeoglu A, Kubilus JK, Yang L, Ferrante KL, Hersch SM, Beal MF, Ferrante RJ. Creatine therapy provides neuroprotection after onset of clinical symptoms in Huntington's disease transgenic mice. J Neurochem. 2003; 85(6):1359–67. [PubMed: 12787055]

Duan W, Guo Z, Jiang H, Ladenheim B, Xu X, Cadet JL, Mattson MP. Paroxetine retards disease onset and progression in Huntingtin mutant mice. Ann Neurol. 2004; 55(4):590–4. [PubMed: 15048901]

Duan W, Peng Q, Masuda N, Ford E, Tryggestad E, Ladenheim B, Zhao M, Cadet JL, Wong J, Ross CA. Sertraline slows disease progression and increases neurogenesis in N171-82Q mouse model of Huntington's disease. Neurobiol Dis. 2008; 30(3):312–22. [PubMed: 18403212]

Ferrante RJ, Andreassen OA, Dedeoglu A, Ferrante KL, Jenkins BG, Hersch SM, Beal MF. Therapeutic effects of coenzyme Q10 and remacemide in transgenic mouse models of Huntington's disease. J Neurosci. 2002; 22(5):1592–9. [PubMed: 11880489]

Ferrante RJ, Kubilus JK, Lee J, Ryu H, Beesen A, Zucker B, Smith K, Kowall NW, Ratan RR, Luthi-Carter R, Hersch SM. Histone deacetylase inhibition by sodium butyrate chemotherapy ameliorates the neurodegenerative phenotype in Huntington's disease mice. J Neurosci. 2003; 23(28):9418–27. [PubMed: 14561870]

Fitzmaurice, GM.; Laird, NM.; Ware, JH. Applied Longitudinal Analysis. Wiley-IEEE; 2004.

Genovese CR, Lazar NA, Nichols T. Thresholding of statistical maps in functional neuroimaging using the false discovery rate. Neuroimage. 2002; 15(4):870–8. [PubMed: 11906227]

Hersch SM, Ferrante RJ. Translating therapies for Huntington's disease from genetic animal models to clinical trials. NeuroRx. 2004; 1(3):298–306. [PubMed: 15717031]

Iannicola C, Moreno S, Oliverio S, Nardacci R, Ciofi-Luzzatto A, Piacentini M. Early alterations in gene expression and cell morphology in a mouse model of Huntington's disease. J Neurochem. 2000; 75(2):830–9. [PubMed: 10899961]

Jenkins BG, Andreassen OA, Dedeoglu A, Leavitt B, Hayden M, Borchelt D, Ross CA, Ferrante RJ, Beal MF. Effects of CAG repeat length, HTT protein length and protein context on cerebral

metabolism measured using magnetic resonance spectroscopy in transgenic mouse models of Huntington's disease. J Neurochem. 2005; 95(2):553–62. [PubMed: 16135087]

Jevtovic-Todorovic V, Hartman RE, Izumi Y, Benshoff ND, Dikranian K, Zorumski CF, Olney JW, Wozniak DF. Early exposure to common anesthetic agents causes widespread neurodegeneration in the developing rat brain and persistent learning deficits. J Neurosci. 2003; 23(3):876–82. [PubMed: 12574416]

Jones BJ, Roberts DJ. The quantitative measurement of motor inco-ordination in naive mice using an accelerating rod. J Pharm Pharmacol. 1968; 20(4):302–304. [PubMed: 4384609]

Kovacevic N, Henderson JT, Chan E, Lifshitz N, Bishop J, Evans AC, Henkelman RM, Chen XJ. A three-dimensional atlas of the mouse brain with estimates of the average and variability. Cereb Cortex. 2005; 15(5):639–645. [PubMed: 15342433]

Lau JC, Lerch JP, Sled JG, Henkelman RM, Evans AC, Bedell BJ. Longitudinal neuroanatomical changes determined by deformation-based morphometry in a mouse model of Alzheimer's disease. Neuroimage. 2008; 42(1):19–27. [PubMed: 18547819]

Lerch JP, Carroll JB, Spring S, Bertram LN, Schwab C, Hayden MR, Henkelman RM. Automated deformation analysis in the YAC128 Huntington disease mouse model. Neuroimage. 2008; 39(1): 32–9. [PubMed: 17942324]

Liang G, Ward C, Peng J, Zhao Y, Huang B, Wei H. Isoflurane causes greater neurodegeneration than an equivalent exposure of sevoflurane in the developing brain of neonatal mice. Anesthesiology. 2010; 112(6):1325–34. [PubMed: 20460994]

Maheswaran S, Barjat H, Bate ST, Aljabar P, Hill DL, Tilling L, Upton N, James MF, Hajnal JV, Rueckert D. Analysis of serial magnetic resonance images of mouse brains using image registration. Neuroimage. 2009a; 44(3):692–700. [PubMed: 19015039]

Maheswaran S, Barjat H, Rueckert D, Bate ST, Howlett DR, Tilling L, Smart SC, Pohlmann A, Richardson JC, Hartkens T, Hill DL, Upton N, Hajnal JV, James MF. Longitudinal regional brain volume changes quantified in normal aging and Alzheimer's APP x PS1 mice using MRI. Brain Res. 2009b; 1270:19–32. [PubMed: 19272356]

Mangiarini L, Sathasivam K, Seller M, Cozens B, Harper A, Hetherington C, Lawton M, Trottier Y, Lehrach H, Davies SW, Bates GP. Exon 1 of the HD gene with an expanded CAG repeat is sufficient to cause a progressive neurological phenotype in transgenic mice. Cell. 1996; 87(3): 493–506. [PubMed: 8898202]

McDaniel B, Sheng H, Warner DS, Hedlund LW, Benveniste H. Tracking brain volume changes in C57BL/6J and ApoE-deficient mice in a model of neurodegeneration: a 5-week longitudinal micro-MRI study. Neuroimage. 2001; 14(6):1244–55. [PubMed: 11707081]

Menalled LB, Chesselet MF. Mouse models of Huntington's disease. Trends Pharmacol Sci. 2002; 23(1):32–9. [PubMed: 11804649]

Miller MI, Trouve A, Younes L. On the metrics and Euler-Lagrange equations of computational anatomy. Annu Rev Biomed Eng. 2002; 4:375–405. [PubMed: 12117763]

Paulsen JS, Hayden M, Stout JC, Langbehn DR, Aylward E, Ross CA, Guttman M, Nance M, Kieburtz K, Oakes D, Shoulson I, Kayson E, Johnson S, Penziner E. Preparing for preventive clinical trials: the Predict-HD study. Arch Neurol. 2006; 63(6):883–90. [PubMed: 16769871]

Peng Q, Masuda N, Jiang M, Li Q, Zhao M, Ross CA, Duan W. The antidepressant sertraline improves the phenotype, promotes neurogenesis and increases BDNF levels in the R6/2 Huntington's disease mouse model. Exp Neurol. 2008; 210(1):154–63. [PubMed: 18096160]

Pinheiro, JC.; Bates, DM. Mixed Effects Models in S and S-Plus. Springer; 2000.

Ramaswamy S, McBride JL, Kordower JH. Animal models of Huntington's disease. ILAR J. 2007; 48(4):356–73. [PubMed: 17712222]

Roberts TJ, Price J, Williams SC, Modo M. Preservation of striatal tissue and behavioral function after neural stem cell transplantation in a rat model of Huntington's disease. Neuroscience. 2006; 139(4):1187–99. [PubMed: 16517087]

Ross CA, Tabrizi SJ. Huntington's disease: from molecular pathogenesis to clinical treatment. Lancet Neurol. 2011; 10(1):83–98. [PubMed: 21163446]

Sawiak SJ, Wood NI, Williams GB, Morton AJ, Carpenter TA. Use of magnetic resonance imaging for anatomical phenotyping of the R6/2 mouse model of Huntington's disease. Neurobiol Dis. 2009; 33(1):12–9. [PubMed: 18930823]

Saydoff JA, Garcia RA, Browne SE, Liu L, Sheng J, Brenneman D, Hu Z, Cardin S, Gonzalez A, von Borstel RW, Gregorio J, Burr H, Beal MF. Oral uridine pro-drug PN401 is neuroprotective in the R6/2 and N171-82Q mouse models of Huntington's disease. Neurobiol Dis. 2006; 24(3):455–65. [PubMed: 17011205]

Schilling G, Becher MW, Sharp AH, Jinnah HA, Duan K, Kotzuk JA, Slunt HH, Ratovitski T, Cooper JK, Jenkins NA, Copeland NG, Price DL, Ross CA, Borchelt DR. Intranuclear inclusions and neuritic aggregates in transgenic mice expressing a mutant N-terminal fragment of huntingtin. Hum Mol Genet. 1999; 8(3):397–407. [PubMed: 9949199]

Schilling G, Coonfield ML, Ross CA, Borchelt DR. Coenzyme Q10 and remacemide hydrochloride ameliorate motor deficits in a Huntington's disease transgenic mouse model. Neurosci Lett. 2001; 315(3):149–53. [PubMed: 11716985]

Stack EC, Kubilus JK, Smith K, Cormier K, Del Signore SJ, Guelin E, Ryu H, Hersch SM, Ferrante RJ. Chronology of behavioral symptoms and neuropathological sequela in R6/2 Huntington's disease transgenic mice. J Comp Neurol. 2005; 490(4):354–70. [PubMed: 16127709]

Stack EC, Smith KM, Ryu H, Cormier K, Chen M, Hagerty SW, Del Signore SJ, Cudkowicz ME, Friedlander RM, Ferrante RJ. Combination therapy using minocycline and coenzyme Q10 in R6/2 transgenic Huntington's disease mice. Biochim Biophys Acta. 2006; 1762(3):373–80. [PubMed: 16364609]

Tabrizi SJ, Scahill RI, Durr A, Roos RA, Leavitt BR, Jones R, Landwehrmeyer GB, Fox NC, Johnson H, Hicks SL, Kennard C, Craufurd D, Frost C, Langbehn DR, Reilmann R, Stout JC. Biological and clinical changes in premanifest and early stage Huntington's disease in the TRACK-HD study: the 12-month longitudinal analysis. Lancet Neurol. 2010; 10(1):31–42. [PubMed: 21130037]

Toga AW, Thompson PM. Temporal dynamics of brain anatomy. Annu Rev Biomed Eng. 2003; 5:119–45. [PubMed: 14527311]

Turmaine M, Raza A, Mahal A, Mangiarini L, Bates GP, Davies SW. Nonapoptotic neurodegeneration in a transgenic mouse model of Huntington's disease. Proc Natl Acad Sci U S A. 2000; 97(14): 8093–7. [PubMed: 10869421]

Vonsattel JP, Myers RH, Stevens TJ, Ferrante RJ, Bird ED, Richardson EP Jr. Neuropathological classification of Huntington's disease. J Neuropathol Exp Neurol. 1985; 44(6):559–77. [PubMed: 2932539]

Walker FO. Huntington's disease. Lancet. 2007; 369(9557):218–28. [PubMed: 17240289]

Ward BC, Agarwal S, Wang K, Berger-Sweeney J, Kolodny NH. Longitudinal brain MRI study in a mouse model of Rett Syndrome and the effects of choline. Neurobiol Dis. 2008; 31(1):110–9. [PubMed: 18571096]

Wingert F. Biometrical analysis of growth functions of cerebral component parts and body weight. J Hirnforsch. 1969; 11(1):133–97. [PubMed: 4903435]

Zhang J, Peng Q, Li Q, Jahanshad N, Hou Z, Jiang M, Masuda N, Langbehn DR, Miller MI, Mori S, Ross CA, Duan W. Longitudinal characterization of brain atrophy of a Huntington's disease mouse model by automated morphological analyses of magnetic resonance images. Neuroimage. 2009; 49(3):2340–51. [PubMed: 19850133]

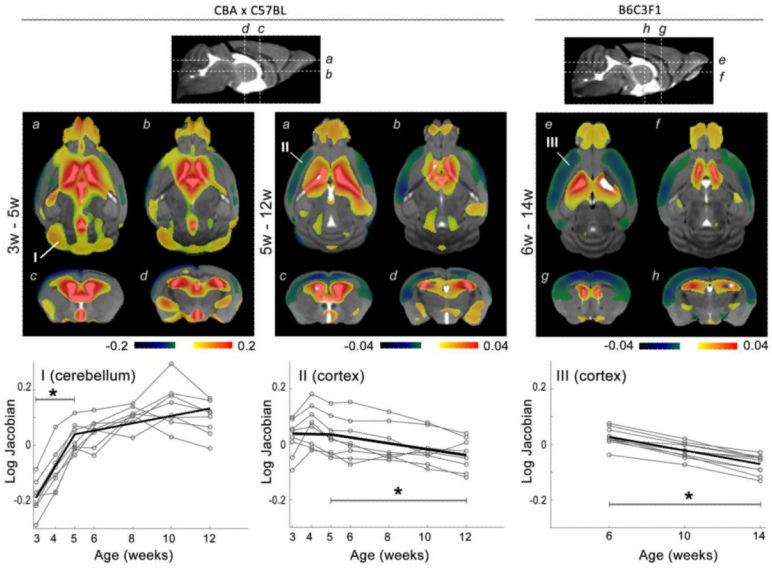

Fig. 1.

Longitudinal changes in the wild-type mouse brains. The color-coded maps show rate of local tissue volume change (measured by log-Jacobian) obtained by the linear mixed effects (LME) modeling overlaid on the reference brain atlas. Only regions with statistically significant (false discovery rate = 0.05) age-related changes within different age spans in the CBA × C57BL/6 and B6C3F1 strains are shown. Plots of log-Jacobian at selected voxel locations within the cerebellum and cortex show the individual trajectories (open circles) and the overall growth curves estimated by the LME model fitting (bold lines). * indicates statistical significance after correction for multiple comparisons with false discovery rate (FDR) set at 0.05.

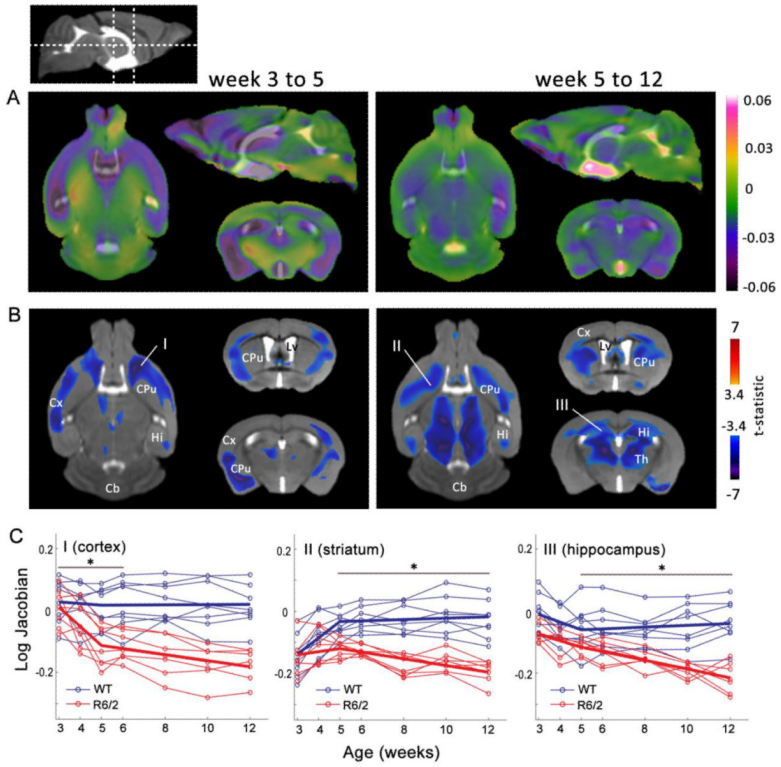

Fig. 2.

Spatiotemporally-varying rate of atrophy in the R6/2 mouse model of HD. A) Color-coded maps showing the average rate of atrophy in the week 3 to 5 and week 5 to 12 age spans are overlaid on orthogonal sections from the reference atlas. The color bar represents the difference in fitted slopes of log-Jacobian between the R6/2 and wild-type control cohorts, with negative values indicating progressive atrophy in the R6/2 brain compared to controls. B) Statistical maps (false discovery rate=0.05) showing regions with significant differences in the fitted slopes of log-Jacobian between the R6/2 and control brains overlaid on the reference atlas. The log-Jacobian profiles at selected voxel locations are plotted in (C), showing the individual trajectories (open circles) and the overall LME model fit (bold lines) for the wild-type (WT) and R6/2 cohorts. Structural abbreviations are: Cx: cerebral cortex, Cb: cerebellum, CPu: striatum, Hi: hippocampus, LV: lateral ventricle, Th: thalamus.

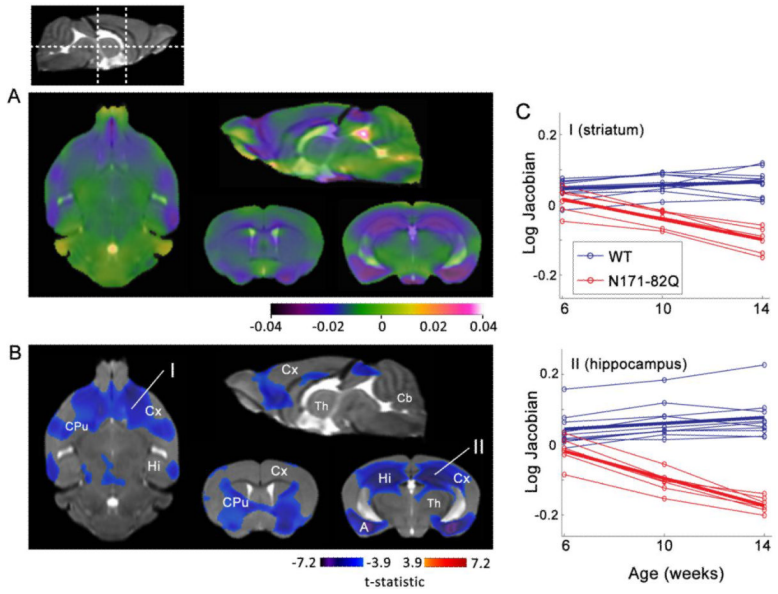

Fig. 3.

Spatiotemporal progression of brain atrophy in the N171-82Q mouse model of HD. A) Maps showing the average rate of atrophy in the N171-82Q mouse brain. The color bar represents the difference in fitted slopes of log-Jacobian between the N171-82Q and wild-type cohorts, with negative values indicating progressive atrophy in the N171-82Q brain compared to controls. Anatomical locations of the sections are indicated in the scout image of the mid-sagittal section. B) Statistical maps (false discovery rate=0.05) showing regions with significant differences in the fitted slopes of log-Jacobian between N171-82Q and control brains overlaid on the reference atlas. The log-Jacobian profiles of the N171-82Q and wild-type (WT) cohorts at the indicated voxel locations are plotted in (C), with the bold lines representing the overall LME model fit. Structural abbreviations are: A: amygdala, Cb: cerebellum, Cx: cerebral cortex, CPu: striatum, Hi: hippocampus, Th: thalamus.

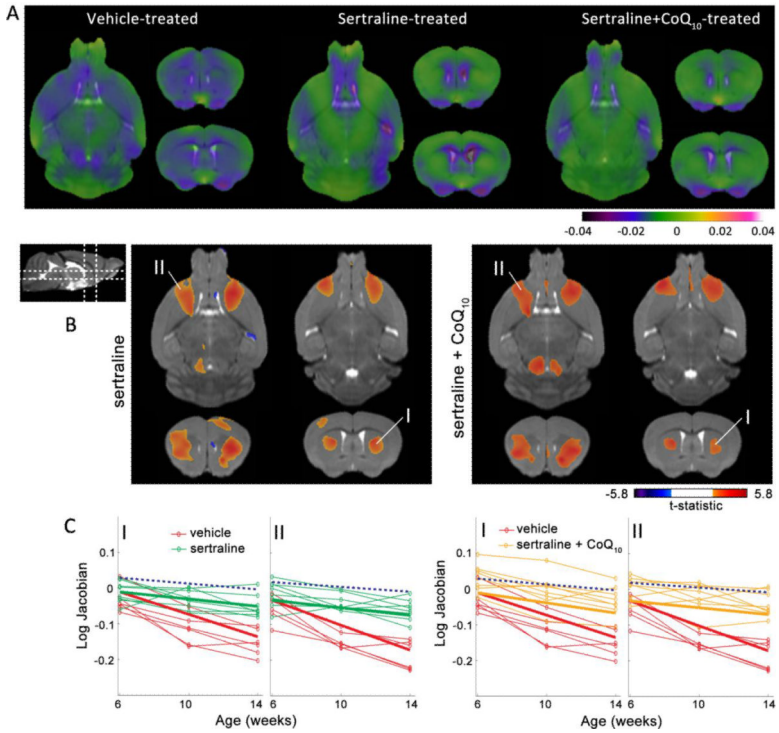

Fig. 4.

Effects of sertraline and combination of sertraline + coenzyme Q_{10} (CoQ_{10}) treatments on the rate of progressive brain atrophy in the N171-82Q model of HD. A) Color-coded maps showing the average rates of atrophy from 6 to 14 weeks of age are overlaid on the reference atlas. Color-bar indicates the differences in fitted slopes of log-Jacobian between vehicle-, sertraline- or combination-treated groups and the wild-type control group. A) Statistical maps (false discovery rate = 0.05), showing regions with significant longitudinal differences between the treatment and sham (vehicle-treated) groups, with positive values of the t-score indicating lower rates of atrophy in the treatment groups. Log-Jacobian profiles at the indicated voxel locations are plotted in (B), with the bold lines indicating the overall linear mixed effects (LME) model fits for the treatment and sham groups. Blue dashed lines indicate the LME model fit for the wild-type control cohort.

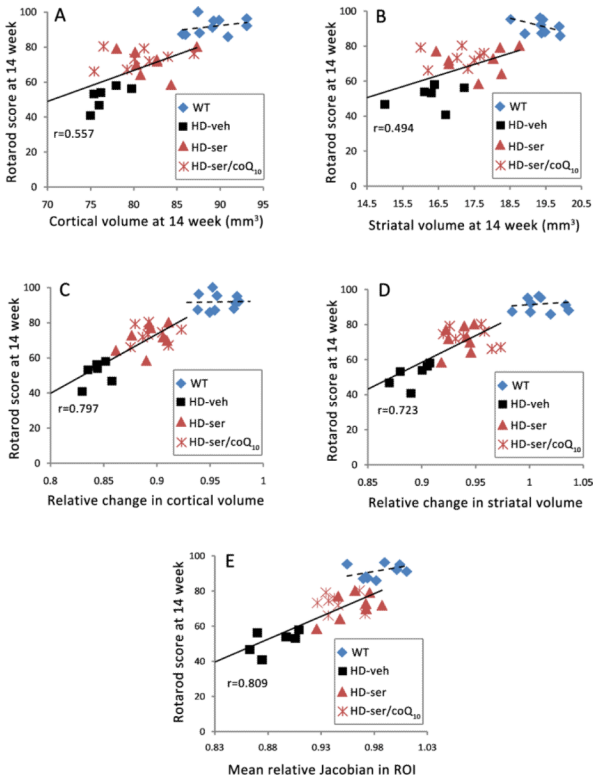

Fig. 5.

Scatter plots showing the relationship between rotarod performance (latency to fall in seconds) and MRI-based volumetric measures in the N171-82Q HD mice. A, B) The rotarod scores at 14 weeks were positively correlated with cortical and striatal volumes at 14 weeks in N171-82Q mice (solid lines, r=0.557, p=0.007 and r=0.494, p=0.02, respectively), but not in wild-type mice (dashed lines). C, D, E) The 14 week rotarod scores showed a stronger correlation with the relative change in cortical and striatal volumes from 6 to 14 weeks (volume at 14 weeks normalized with respect to volume at 6 weeks) (r=0.797, p<0.001and r=0.723, p<0.001, respectively); and with the mean change in Jacobian within a region of interest (ROI) in the frontal cortex and striatum that showed significant treatment effects on the rate of atrophy (r=0.809, p<0.001). Each data point represents one subject, with the color indicating the genotype and treatment group: wild-type (WT) controls, and N171-82Q transgenic HD mice treated with vehicle (HD-veh), sertraline (HD-ser) or combination of sertraline and coenzyme Q_{10} (HD-ser/coQ_{10}).

Table 1

Cohort sizes and time points for serial in vivo MRI scans for the R6/2 and N171–82Q models of HD used in the study

	Genotype / Treatment	Number of subjects	Time points for in vivo MRI (age in weeks)
R6/2 study	Wild-type (control)	n=8	3, 4, 5, 6, 8, 10, 12
	R6/2	n=7	3, 4, 5, 6, 8, 10, 12
N171–82Q study	Wild-type (control)	n=10	6, 10, 14
	N171–82Q / vehicle	n=6	6, 10, 14
	N171–82Q / coenzyme Q_{10}	n=6	6, 10, 14
	N171–82Q / sertraline	n=8	6, 10, 14
	N171–82Q / sertraline + coenzyme Q_{10}	n=8	6, 10, 14